Next Nanotechnology 8 (2025) 100210

Contents lists available at ScienceDirect

Next Nanotechnology

journal homepage: www.sciencedirect.com/journal/next-nanotechnology

Research article

Phytochemical mediated zinc oxide nanoparticles from *Euphorbia antiquorum*: Synthesis, characterization & antibacterial activity

Surya Sivakumar [a], Boobal Rangaswamy [a,*,1], Lathika Shanmugam [a,2], Kamalesh Marudhachalam [a,b]

[a] Department of Biotechnology, PSG College of Arts & Science, Coimbatore, Tamil Nadu 641014, India
[b] Department of Human Genetics and Molecular Biology, Bharathiar University, Coimbatore, Tamil Nadu 641046, India

ARTICLE INFO

Keywords:
Nanoparticles
ZnO
Green synthesis
Antibacterial activity

ABSTRACT

The plant extract of *Euphorbia antiquorum* was utilized to perform a green synthesis of zinc oxide nanoparticles (ZnO NPs). The phytochemical components of the nanoparticles were subsequently examined. The ZnO NPs produced through biosynthesis were analyzed using several spectroscopic methods. The plant extract revealed the existence of alkaloids, tannins, flavonoids, terpenoids, gums, and mucilages, which played a role in the production of ZnO NPs by decreasing metal ions and ensuring the stability of the process. The Fourier-transform infrared spectroscopy (FTIR) revealed the unique spectra associated with ZnO NPs at a wavenumber of 455.20 cm^{-1}. The nanoparticles were observed to have a nanoflake structure by analysis with the Field Emission Scanning Electron Microscope (FE-SEM). The average size of the crystallites was determined to be 37 nm using X-ray diffraction (XRD) patterns. The Energy-dispersive X-ray spectroscopy (EDX) spectra of ZnO NPs confirmed the nanoparticles production with very few impurities. The antibacterial efficacy of the synthesized NPs was assessed by determining the Minimum Inhibitory Concentration (MIC) and Minimum Bacterial Concentration (MBC) against *E. coli, Pseudomonas* sp., *Vibrio* sp., and *Bacillus* sp. The presence of phytochemicals and the activity against microorganisms evidenced the importance of NPs to prevent infection, promote wound healing and to treat diseases. This study determines that ZnO NPs possess substantial antibacterial properties against diverse aquatic pathogens, presenting them as a viable substitute for conventional antibiotics.

1. Introduction

Nanotechnology significantly impacts various fields, including healthcare, agriculture, electronics, and environmental remediation [1]. It enables precise drug delivery, minimizing failure and rejection risks, and is effective in treating inflammatory, infectious, bone, cardiovascular, and pulmonary diseases [2,3]. Nanoparticles, conjugated with antibodies via polyethylene glycol, are used in breast cancer therapy [4,5]. Additionally, it offers an environmentally acceptable method for contamination removal through green synthetic nanoparticles without chemicals [6,7]. The eco-friendly production of precious metals has positive impacts on human well-being and the natural surroundings [8].

Green synthesis extracts and preserves plant-derived biomolecules like enzymes, polyphenols, proteins, flavonoids, and terpenoids for pharmaceutical applications, where they act as catalysts, reducing agents, stabilizers, or capping agents [9–11]. It minimizes environmental contamination by utilizing natural reducing agents and solid wastes, reducing greenhouse gas emissions while addressing agricultural and industrial waste concerns to promote ecological balance [12]. Additionally, green-synthesized nanoparticles, including cerium oxide, exhibit anti-inflammatory properties, biocompatibility, and cost-effectiveness, making them suitable for antimicrobial therapy, wound healing, drug delivery, disease diagnostics, electrochemical sensing, and corrosion protection [13–16].

The Euphorbiaceae family is the most extensive group of plants, consisting of 300 genera and around 7500 species. *E. antiquorum* produces a latex that belongs to the Euphorbiaceae family. This latex contains active components and is commonly utilized for therapeutic purposes [9–11]. The utilization of *E. antiquorum* for the ZnO NPs synthesis represents significant progress in the advancement of

* Corresponding author.
E-mail address: boobal@psgcas.ac.in (B. Rangaswamy).
[1] Orcid: 0000–0002-8270–9755
[2] Orcid: 0009–0006-1322–4515

https://doi.org/10.1016/j.nxnano.2025.100210
Received 22 January 2025; Received in revised form 28 June 2025; Accepted 30 June 2025
Available online 9 July 2025

nanotechnology. This approach offers an environmentally benign, biocompatible, and versatile way of producing nanoparticles, which can be applied across multiple industries. This technology provides a sustainable option to conventional methods of producing nanoparticles [17] by using the bioactive features of *E. antiquorum* instead of chemical precursors [18] that can be detrimental to the environment. ZnO is a type of semiconductor that is highly adaptable because of its ability to allow light to pass through it and its ability to emit light [19]. Phytochemicals derived from plants have a significant role in the synthesis of metal oxide nanoparticles such as ZnO, CuO, and Ag. They serve to reduce the metal ions while stabilizing the entire process [20]. Nanoparticles are utilized for the purpose of combating insect pests and herbivore attacks [21]. ZnO NPs are employed for several applications including antibacterial, biomedical, agriculture, cosmetics, and biofertilizers [22]. ZnO NPs are typically produced using several physical and chemical techniques, including ultrasonic conditions, chemical vapor deposition, sol-gel, spray pyrolysis, microwave-assisted methods, hydrothermal, and precipitation processes [23,24]. The ZnO NPs produced by *E. jatropa* latex function as reducing agents and also reduce the size of crystallites, resulting in changes to the electrical, optical, and sensing characteristics of nanopowders [25]. The unique characterization of nanoparticles in relation to the features of different species of *Euphorbia* plants and their diverse applications. Previous research has found that different *Euphorbia* plant species such as *E. hirta*, *E. milii*, and *E. Petiolata,* have been utilized for environmental applications [26–29].

In biomedical and biological applications, nanoparticles synthesized from various *Euphorbia* plant species, including *E. confinalis, E. milii, E. dendroides, E. acruensis, E. antiquorum L., E. hirta, E. wallichii, E. pseudocactus Berger, E. tirucalli, E. retusa, E. serpens, E. jatropa, E. helioscopia L.,* and *E. dracunculoides*, have shown potential for therapeutic use [30, 25,31–45]. Recent research on *E. antiquorum* has focused on utilizing green synthesis to create gold nanoparticles (AuNPs) with antioxidant and anticancer effects [46]. The silver nanoparticles (AgNPs) derived from *E. antiquorum* have demonstrated promising capabilities in the fields of anticancer, antibacterial, and larvicidal activities, suggesting their potential biological applications in the development of nanoformulations [30]. Previously, the methanolic extract of *E. wallichii* was used to create AgNPs, which effectively inhibited the chosen pathogens (*A. fumigatus* and *S. aureus*) [47]. The AuNPs produced using ethanol extract from *E. peplus* leaves have anti-cancer properties [48].

ZnO NPs are increasingly utilized to target microorganisms responsible for infections and environmental contamination. They exhibit strong antimicrobial properties by interacting with microbial cell membranes, leading to cell wall disruption and bacterial death. ZnO NPs synthesized using *E. antiquorum* have demonstrated enhanced antibacterial activity, with bioactive compounds in the plant extract contributing to their efficacy against *E. coli, Vibrio sp., Pseudomonas sp.,* and *Bacillus sp.*, making them valuable for food packaging, preservation, and medical applications [49–51].

In cancer therapy, ZnO NPs induce cytotoxic effects by generating reactive oxygen species (ROS), which cause oxidative stress in cancer cells. This oxidative stress damages cellular components such as DNA, proteins, and lipids, ultimately triggering apoptosis, or programmed cell death. Studies have shown that ZnO NPs synthesized using *E. antiquorum* extracts exhibit significant anticancer activity, particularly against human breast cancer (MCF-7) cells, by increasing ROS levels and activating apoptotic pathways [52,53]. Additionally, green-synthesized ZnO NPs offer benefits such as improved stability and surface area, enhancing their potential applications in drug delivery, catalysis, environmental remediation, and sensor technology [54]. Current advancements focus on utilizing plant-derived reducing agents to optimize ZnO NPs synthesis for applications in biomedical, textile, and environmental sectors.

The synthesis of ZnO NPs was conducted utilizing a plant extract derived from *E. antiquorum*. The properties of the produced nanoparticles were analyzed using a variety of methods. The morphological and structural properties of the produced ZnO NPs were validated using techniques such as FT-IR, XRD, EDX, and FE-SEM. The current study assesses the antibacterial efficacy of ZnO NPs against aquatic pathogens utilizing MIC and MBC assays. As far as we know, this is the initial documentation on the production of ZnO NPs using *E. antiquorum*.

2. Materials and methods

2.1. Sample preparation

The sample of *E. antiquorum* was obtained from Salem, Tamil Nadu for the purpose of conducting green synthesis. The collection was authenticated by the Botanical Survey of India, with the authentication number BSI/SRC/5/23/2023–24/Tech-115. At first, the plant spines were delicately removed. The plant was dissected longitudinally and carefully transferred into the beaker. Subsequently, the accumulated white substance was measured to be 6 g and then poured into 100 milliliters of distilled water. Then, the mixture was thoroughly blended and heated to a temperature ranging from 60 ℃ to 80 ℃.

2.2. Biosynthesis of nanoparticles

To synthesize nanoparticles, an appropriate precursor Zinc nitrate solution was prepared. A 5 g sample was combined with 100 mL of distilled water and introduced into the solution containing 0.1 M of zinc nitrate. The solution was set in a magnetic stirrer for a while to reach 70 ℃ for 30 min. The plant extract and zinc nitrate solution were combined in a 1:1 ratio and heated to a temperature of 80 ℃ for 15 min in order to fully dissolve the zinc nitrate. The pH of the solution was adjusted to 8.4 to promote ZnO precipitation. The precipitation was initiated by the addition of NaOH pellets. The reaction mixture was stirred at room temperature for a few hours until the formation of a white precipitate was observed. The extract was centrifuged for 10 min at 8000 rpm. The pellet was then cleansed with ethanol to remove any impurities and the purified ZnO precipitate was dried in a hot air oven at 100 °C to obtain biosynthesized ZnO NPs [55]. The sample was sent for characterization in order to confirm the existence of the nanoparticles.

2.3. Qualitative analysis of phytochemicals

E. antiquorum was to identify the presence of tannins, flavonoids, saponins, alkaloids, phytosterols, terpenoids, gums, and mucilages. In order to detect the presence of alkaloids, a solution containing 2 g of iodine and potassium iodide in 100 mL of distilled water was prepared. The sample was treated with small quantity of hydrochloric acid and filtered. The formation of a reddish-brown solid was induced by the addition of Wagner's reagent [56]. Flavonoids were detected in the samples using Shinoda's assay [57]. Shinoda's test was conducted, where the extract was combined with zinc powder, and concentrated sodium hydroxide was introduced slowly and in small amounts. Flavonoids can be detected by the appearance of a vivid red hue. The presence of tannins was established by the $FeCl_3$ Test. When 2 mL of the extract was combined with a 5 % $FeCl_3$ solution, it resulted in a violet tint. Conversely, when mixed with a 10 % lead acetate solution, a white precipitate was formed. The occurrence of tannins was detected through the production of a black tint. The combination of extracts, chloroform, and concentrated sulfuric acid in Salkowski's test resulted in a reddish-brown tint, indicating the presence of terpenoids in the extracts [58]. Phytosterols were detected through the utilization of Salkowski's assay. Each sample was put separately to 5 mL of chloroform solutions containing strong sulfuric acid, and no brown staining was observed.

The Liebermann-Burchard test was conducted to determine the presence of phytosterols in the extract. This was achieved by adding chloroform to the extract together with concentrated sulfuric acid and dilute acetic acid, resulting in the appearance of a brownish-green color [57].

In order to conduct the saponins test, 2 mL of extract was combined with 10 mL of distilled water and subjected to progressive heating and shaking for a duration of 5 min. The existence of saponins was determined by the long-lasting foam generation. The presence of gums and mucilages was identified by combining the extract with 25 mL of pure alcohol, continuously agitating, and subsequently filtering. The precipitate was dried by exposure to air and subsequently analyzed for its ability to expand [56].

2.4. Characterization of ZnO NPs

2.4.1. XRD

XRD analyses were performed on ZnO NPs synthesized using *E. antiquorum* to investigate their structural characteristics and assess their phase composition. The X-ray diffractometer utilized in this study was PAN Analytical X′ Pert PRO XRD PW 3040, which operated with CuKα radiation at a wavelength of 1.5406 Å. The instrument had an accelerating voltage of 45 kV and a current of 30 mA [59]. The XRD pattern was obtained by irradiating the sample at 2θ angles ranging from 10 to 80° while it was positioned on a metal holder. The scanning velocity ranged from 0.01 to 0.08 steps per second, with increments of 0.03°. The Scherrer formula was employed to determine the particle size of the samples. A distinct diffraction peak signifies a high degree of crystallinity in the particles. As revealed through Bragg's law [60],

$$n\lambda = 2d\sin\theta$$

The Scherrer Eq. [1] is the first technique that established the relationship between crystallite size and peak broadening [61].

$$\text{Crystallite size, } D_s = K\lambda/\beta.\cos\theta \quad (1)$$

In this Eq. [2], D indicates crystallite size, β_{hkl} is full-width half maximum (in radian), K is 0.9 dimensionless constant and θ is the Bragg angle.

$$d_{hkl} = \frac{1}{\sqrt{4/3(h^2+k^2+hk)+ \quad l^2/c^2}} \quad (2)$$

The unit cell parameter 'a' for the (100) plane is obtained from [62]

$$a = \frac{\lambda}{\sqrt{3}\sin\theta_{(100)}} \quad (2a)$$

The unit cell parameter 'c' for the (101) plane is determined from [59], [62]

$$c = \frac{\lambda}{\sin\theta_{(101)}} \quad (2b)$$

The volume V is obtained from [60]

$$V = \frac{\sqrt{3}a^2c}{2} \quad (3)$$

2.4.2. FT-IR

FTIR spectroscopy was employed to identify putative functional groups present during nanoparticle production and to analyze the chemical composition. The desiccated material was mixed with KBr pellets in a proportion of 1:100, and subsequently compressed into a clear and slender pellet [63] FTIR spectra were acquired at room temperature, with a spectral resolution of 4 cm^{-1}, covering the range from 4000 to 400 cm^{-1}.

2.4.3. EDX and FE-SEM

The size and shape of the nanoparticles have been observed using a FE-SEM. The elemental composition of the nanoparticles was determined using EDX analysis. The EDX data and FE-SEM pictures were obtained using a Hitachi S-3400N spectrometer [63].

2.5. Antibacterial assay

The antibacterial efficacy of ZnO NPs in combination with plant extract was evaluated against *E. coli, Pseudomonas sp., Vibrio sp*. and *Bacillus sp.* bacteria was determined by MIC assay. The 96-well plates were incubated at 37 °C for 24 h with two-fold dilutions of ZnO NPs having concentrations ranging from 2500 to 78.125 μg/mL. The MIC of ZnO NPs against microorganisms was determined at 600 nm via UV–Vis spectrophotometer. The MBC assay was used to confirm bacterial suppression in the wells. It was then filtered and cooled down to room temperature. Petri plates with well contents were left to incubate at 37 °C for 24 h [64]. The results obtained were subjected to statistical analysis using the One-Way ANOVA test.

3. Results

3.1. Qualitative analysis of phytochemicals

The phytochemical screening **(**Table 1**)** confirmed the presence of alkaloids, terpenoids, flavonoids, tannins, and gums/mucilages, playing a crucial role in nanoparticle synthesis as reducing and stabilizing agents. The absence of phytosterols and saponins suggests the involvement of other bioactive compounds in ZnO NP formation.

3.2. Characterization of ZnO NPs

3.2.1. XRD

The X-ray wavelength is denoted by λ (0.154 nm), d demonstrates the spacing between the planes with Miller indices (h, k, l), and n refers to the diffraction order. The d value for the hexagonal structure of ZnO was determined using the equation (61). The X-ray diffraction (XRD) peaks were detected at specific angles, known as 2θ values. The observed 2θ values for the peaks were 26.15, 32.96, 36.45, 44.02, 47.74, 59.17, and 67.94 degrees. The produced nanoparticles exhibited diffraction peaks corresponding to the (100), (002), (101), (102), (110), (103), (112), and (202) lattice planes of the hexagonal wurtzite structure, as shown in Fig. 1a, b. The average crystalline size obtained using Scherrer's technique is 37 nm, as indicated in Table 2 and calculated using Eq. [1]. XRD analysis **(**Table 2**)** revealed diffraction peaks corresponding to ZnO NPs' hexagonal wurtzite structure. The crystallite size ranged from 23.95 nm to 63.73 nm, with the most intense peak at 32.96° (2θ), corresponding to 63.73 nm, indicating high crystallinity. The d-spacing values further supported the structural integrity of the synthesized ZnO NPs. The lattice parameters for ZnO, as presented in Table 3, were calculated as a = 0.04 Å, c = 0.277 Å, and a c/a ratio of 6.9, confirming the hexagonal structure using Eqs. (2), (2a), [2b] and [3].

3.2.2. FT-IR

FT-IR spectroscopy was conducted to find several functional groups present on the surface of ZnO NPs without leaf extract and with leaf extract. The functional groups present in the synthesized ZnO sample and plant extract were identified using an FT-IR instrument, and the results were displayed in a plot **(**Fig. 2**a, b)**. The plant extract's spectrum exhibits 9 peaks, which can be used to identify the chemical compounds that correspond to the standard IR for capping and reducing. The plant

Table 1
Phytochemical screening of green synthesized ZnO NPs.

Phytochemicals	Results
Phytosterols	Absent
Alkaloids	Present
Terpenoids	Present
Flavonoids	Present
Tannins	Present
Gums and Mucilages	Present
Saponins	Absent

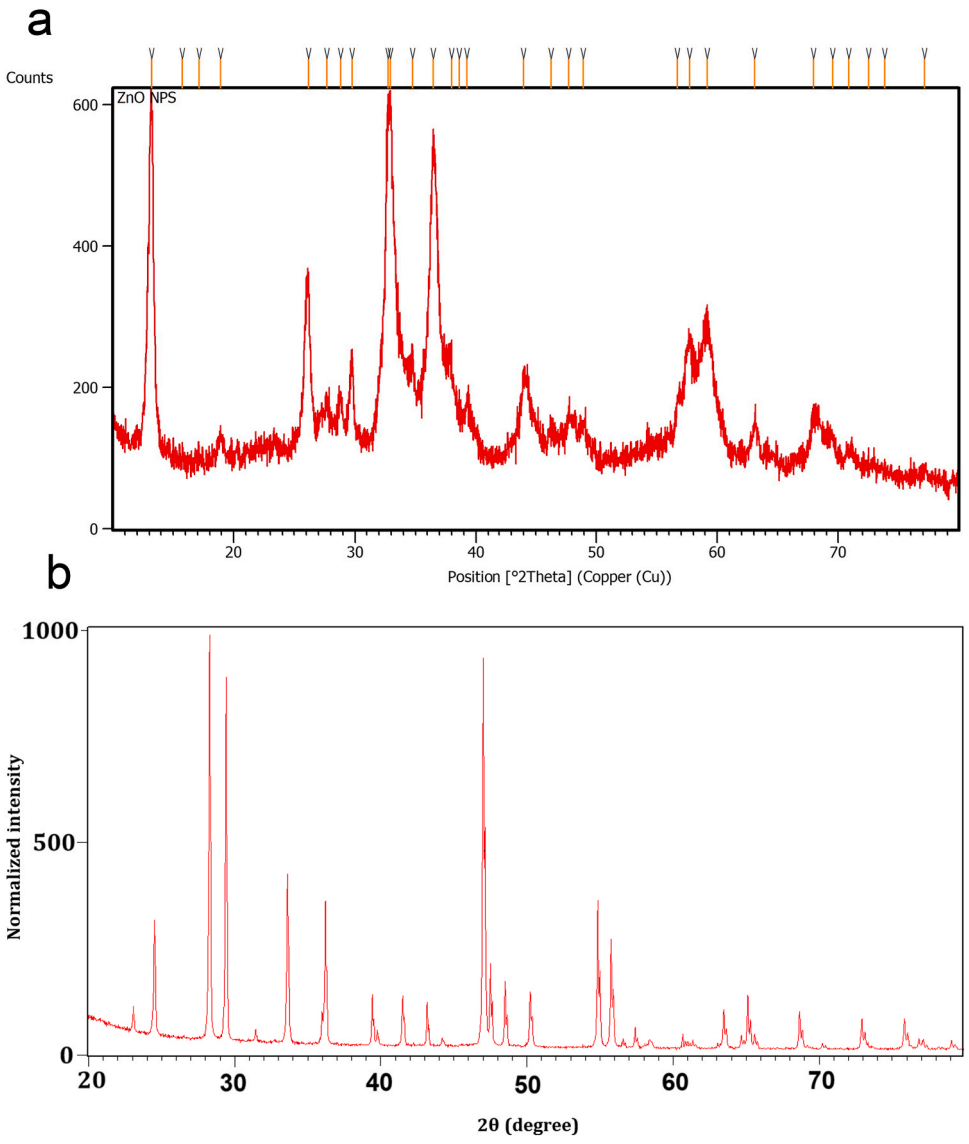

Fig. 1. XRD analysis of ZnO NPs. **a** Normalized intensity of XRD peak analysis.

Table 2
Characterization and crystallite size of ZnO NPs obtained from XRD analysis.

2θ	FWHM	d-spacing (nm)	Intensity	Crystallite size (nm)
26.15	0.26	3.4	46.36	31.37
32.96	0.13	2.71	96.13	63.73
36.45	0.16	2.46	85.94	52.27
44.02	0.33	2.05	22.2	25.97
47.74	0.26	1.9	13.48	33.41
59.17	0.33	1.5	35.32	27.68
67.94	0.4	1.37	14.53	23.95

Table 3
Lattice parameters of ZnO NPs.

hkl	d_{hkl} (Å)	Lattice parameters (Å)	c/a ratio	V (Å^3)
100	0.16	a = 0.04		0.0003
101	1.16	c = 0.277	c/a = 6.9	

extract of *E. antiquorum* mediated ZnO NPs exhibits peaks in its spectra at wavelengths of 455.20 cm^{-1}, 486.06 cm^{-1}, 509.29 cm^{-1}, 540.07 cm^{-1}, 648.08 cm^{-1}, 686.66 cm^{-1}, 1010.70 cm^{-1}, 1327.03 cm^{-1}, and 1489.05 cm^{-1}. The plant extract of *E. antiquorum* exhibits common significant peaks at 648.08 cm^{-1} and 1010.70 cm^{-1}. The FT-IR spectrum of ZnO NPs exhibited a peak at a wavenumber of 455.20 cm^{-1}. The sulfone molecule has S═O stretching bonds, as evidenced by the prominent peak at a wavenumber of 1327.03 cm^{-1}. The prominent peak observed at wavenumbers between 500 cm^{-1} and 1400 cm^{-1} is associated with the stretching vibration of C-I and C-F bonds in halogen and fluoro compounds. The presence of the C-F stretch in ZnO NPs was detected by a distinct peak at 1010.7 cm^{-1} corresponding to the typical functional groups. The C═O stretch, which indicates the existence of an alkene, was found at 686.6 cm^{-1}. Additionally, the C-Br stretch was identified by a prominent band at 540 cm^{-1}. The band observed at a wavenumber of 1489.05 cm^{-1} was determined to correspond to the alkane functional group, namely the vibration of C-H stretching.

3.2.3. FE-SEM

The FE-SEM technique was employed to examine the structure, dimensions, arrangement, and physical characteristics of the produced ZnO NPs. Fig. 3 depicts the FE-SEM images of ZnO NPs. The particle diameters were measured using ImageJ software. The morphology of the extracts was modified by the calcination temperature of 300 °C. The

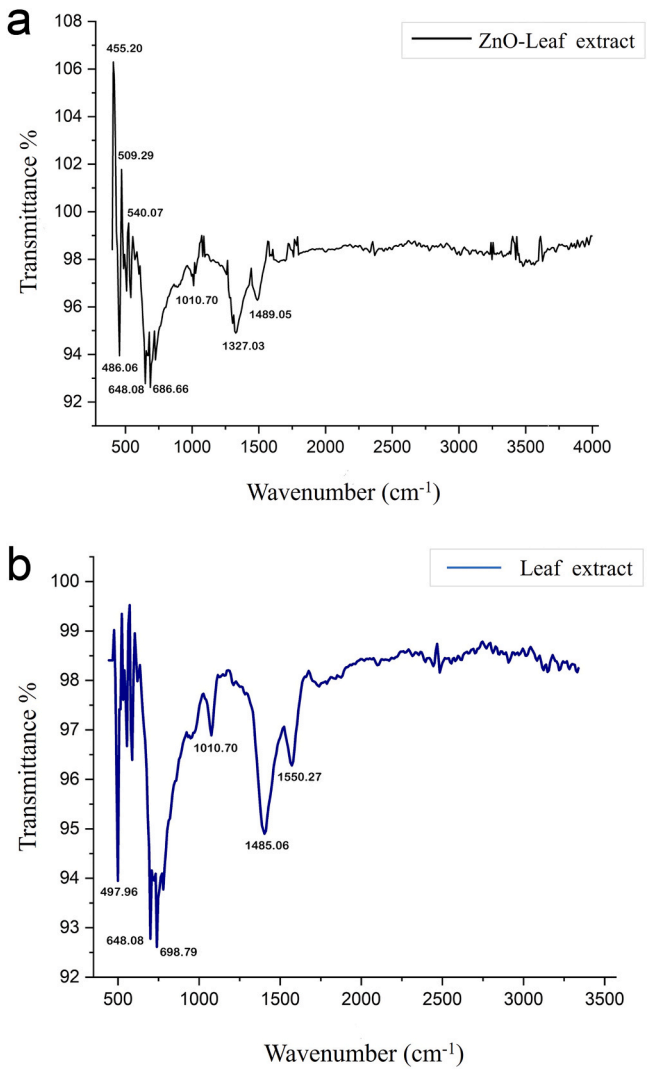

Fig. 2. FT-IR spectra of the green synthesized ZnO NPs a) Leaf extract b) ZnO NP-leaf extract.

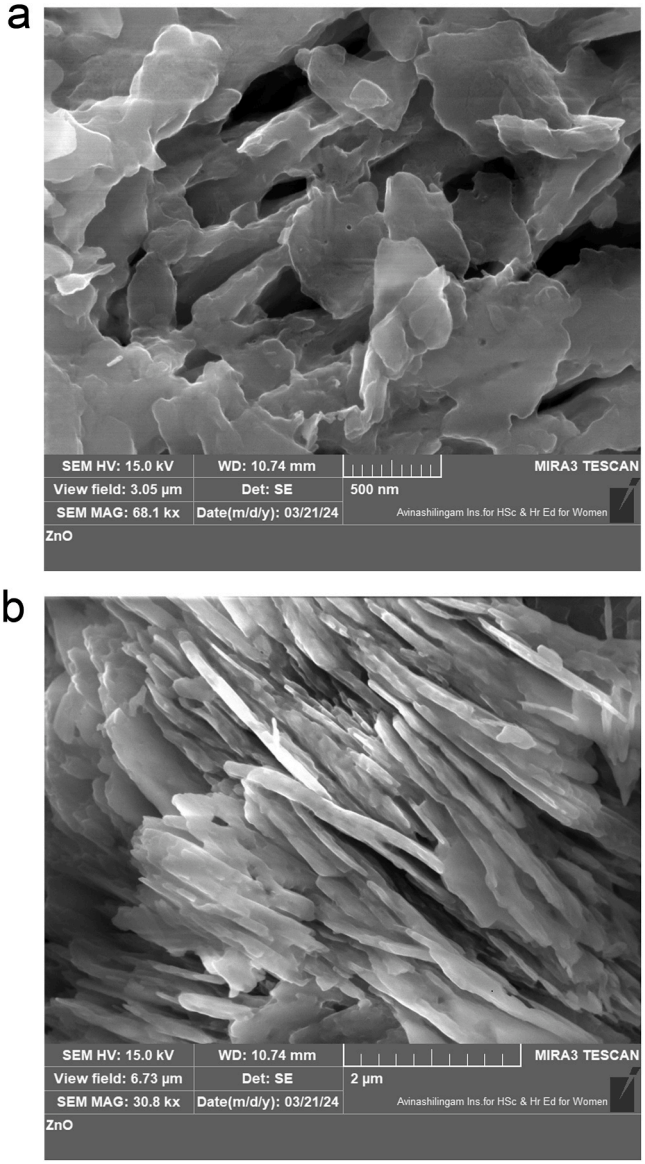

Fig. 3. FE-SEM image of synthesized ZnO NPs (a) 500 nm (b) 2 µm.

ZnO NPs were observed in the form of nanoflakes and the size of the nanoparticles ranged from 56 nm for particles with a size of 500 nm to 16 nm for particles with a size of 2 µm **(**Fig. 3**).**

3.2.4. EDX

The elemental composition of ZnO NPs produced from *E. antiquorum* extract was assessed by EDX analysis. The EDX analysis identified five distinct peaks that corresponded to signals of zinc, carbon, and oxygen. These findings offer further evidence for the formation of ZnO NPs, as depicted in Fig. 4. The peaks correspond to the optical absorption of the nanoparticle. The nanoparticle elemental composition examination indicated a high level of purity, with Carbon comprising 16 %, Zinc comprising 21 %, and Oxygen comprising 64 %. Table 4 provides a visual representation of the minimum impurities present. The EDX spectra of the green-produced ZnO NPs display prominent signals originating from Zn and O elements while exhibiting less pronounced signals from C elements.

3.3. Antibacterial assay

As shown in Table 5, the zone of inhibition for *Vibrio* sp. and *Bacillus* sp. was observed as 10 mm, while *E. coli* as 12 mm. MBC for *E. coli, Pseudomonas* sp., *Vibrio* sp., and *Bacillus* sp. were 5.8 µg/mL, 4.9 µg/mL, 5.1 µg/mL, 3.4 µg/mL while MIC value of ZnO NPs against food borne pathogen (*Pseudomonas sp.*) were ranged from 3.1 to 5.4 µg/mL. *E. coli* shows greater activity with MIC = 5.4 µg/mL and MBC = 5.8 µg/mL when compared to others **(**Fig. 5**)**. A lower MIC indicates enhanced antibacterial potency. These results indicate that ZnO NPs were more effective in inhibiting the growth of foodborne and environmental pathogens. By using One-way ANOVA, the antibacterial assay results were statistically significant ($P < 0.117$) against ZnO NPs.

4. Discussion

The utilization of plant extracts in the green production of nanoparticles is an economical and ecologically beneficial approach. Plant extracts contain bioactive chemicals and nanoparticles with significant therapeutic effects applicable in various medical fields. In this study, plant extracts of *Euphorbia antiquorum* were used to produce ZnO NPs. Phytochemical analysis is critical for identifying bioactive constituents, contributing to pharmaceutical formulations [65]. The phytoconstituents found in *Euphorbia* species, are widely distributed in Gujarat, India, include tannins, flavonoids, phenolic compounds, terpenoids, and triterpenes. These compounds, as revealed by studies on twelve to thirteen *Euphorbia* species, have medicinal properties and are employed

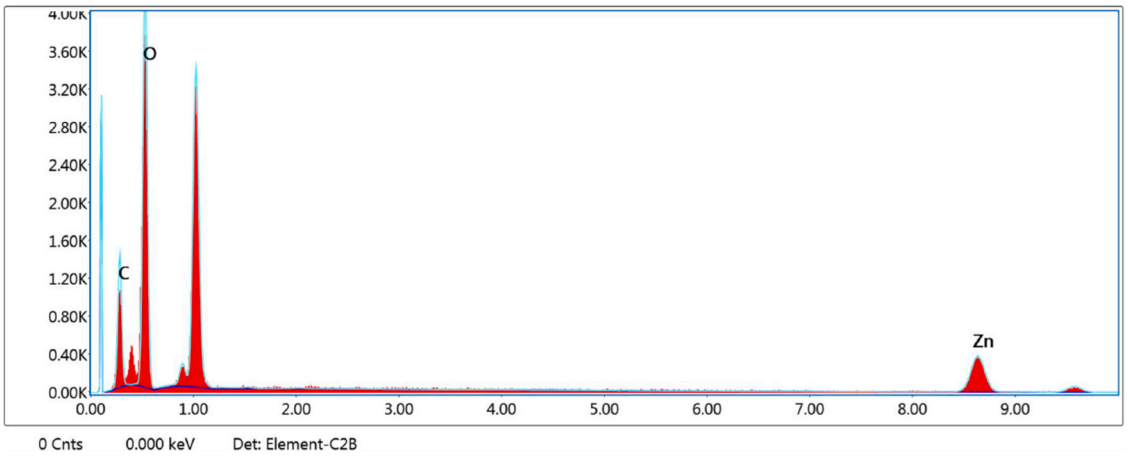

Fig. 4. EDX analysis of green synthesized ZnO NPs.

Table 4
EDX investigation of elemental composition.

Elements	Weight %	Atomic %
C	19.18	37.67
O	29.77	43.9
Zn	51.05	18.43
Total	**100**	**100**

Table 5
Zone of inhibition, MIC, and MBC values for pathogens.

Types of bacteria	Zone of inhibition (Diameter in mm)	Number of tested isolates	MIC (μg/mL)	MBC (μg/mL)
E. coli	12	1	5.4	5.8
Pseudomonas sp.	9	1	3.1	4.9
Vibrio sp.	10	2	4.6	5.1
Bacillus sp.	10	1	3.6	3.4

in treating skin problems, cancer, arthritis, and cytotoxicity [66].

4.1. Qualitative analysis of phytochemicals

The *E. antiquorum* plant specifically contains phytochemicals such as flavonoids, diterpenes, triterpenes, tannins, phenolic compounds, alkaloids, sterols, and terpenoids, which act as stabilizing and reducing agents during ZnO NP synthesis [67];[68]. A similar study by [37] highlighted the presence of alkaloids, tannins, flavonoids and triterpenes in *E. retusa*. Additionally, previous research on *E. heterophylla* and *E. hirta* reported phytochemicals such as flavonoids, saponins, tannins, and alkaloids, aligning with our phytochemical analysis [69];[70]. The therapeutic potential of these phytochemicals is consistent across the *Euphorbiaceae* family [71].

4.2. XRD

The XRD spectra reveal that ZnO calcinated at 700 °C exhibits lattice parameters of a = 3.27 Å and c = 5.26 Å, with an average crystallite size of 53 nm. These findings underscore the impact of calcination temperature on the surface morphology, particle size, and crystallinity of ZnO nanoparticles, corroborating earlier studies [72];[42]. Similarly, the XRD analysis of *Cucumis maderaspatanus* extract-mediated ZnO NPs revealed a crystallite size of 30 nm, further validating its role as a reducing agent in green synthesis [43]. The XRD investigation conducted in this study showed a minor alteration in the lattice parameters (a = 0.04 and c = 0.277 Å) following calcination at 300 °C, with an average crystal size of 37 nm. These structural changes indicate enhanced crystallinity and phase purity, emphasizing the role of calcination in optimizing ZnO NPs' structural properties.

4.3. FT-IR

FTIR analysis provided additional evidence of functional groups involved in nanoparticle stabilization. The presence of C═O stretching vibrations at 1645 and 1639 cm^{-1}, along with C-H stretch vibrations at 1489.05 cm^{-1}, supports the role of biomolecules in capping and stabilizing the NPs [44];[43]. Furthermore, the characteristic ZnO vibration at 422 cm^{-1} affirms the successful synthesis of ZnO NPs, consistent with previous findings [73].

4.4. SEM and EDX

The morphological changes in ZnO NPs due to calcination are evident from SEM images, which display a nanoflake structure at 300 °C. This observation aligns with prior studies highlighting temperature-induced morphological transitions [74]. The XRD, EDX, and SEM analyses collectively confirm the effective synthesis and high purity of ZnO NPs via the green synthesis method.

EDX analysis further validated the synthesized ZnO NPs' elemental composition, revealing 72.27 % zinc and 8.35 % oxygen, closely aligning with synthesized ZnO NPs containing 80.82 % zinc and minor carbon content [75]. The high purity of ZnO NPs is further supported by reports on *E. jatropa* plant-derived NPs, which comprised only Zn and O components [25]. The prior research estimated that the EDX spectrum of *Digera muricata* synthesized ZnO NPs reveals sharp signals of 17.58 % Zinc and 30.49 % oxygen, while comparing the present study shows better results [76]. A recent study found that the *E. antiquorum* plant showed that AgNPs had a 73.22 % inhibitory effect at a concentration of 1000 μg/mL, while copper nanoparticles had a cytotoxic activity of 68.85 % against MCF-7 breast cancer cells [53].

4.5. Antibacterial assay

In terms of biological activity, ZnO NPs synthesized via green methods exhibited significant antibacterial properties against pathogens such as *E. coli*, *Pseudomonas sp.*, *Vibrio sp.*, and *Bacillus sp.* The MIC values ranged from 3.1 to 5.4 μg/mL, consistent with prior studies [77]. The concentration-dependent antibacterial activity was evident as increasing ZnO NP concentrations (5–45 μg/mL) enhanced bacterial growth inhibition [78]. Further, eco-friendly synthesis approaches have shown promising antimicrobial activities. For instance, *E. antiquorum*-mediated AuNPs demonstrated inhibitory effects against

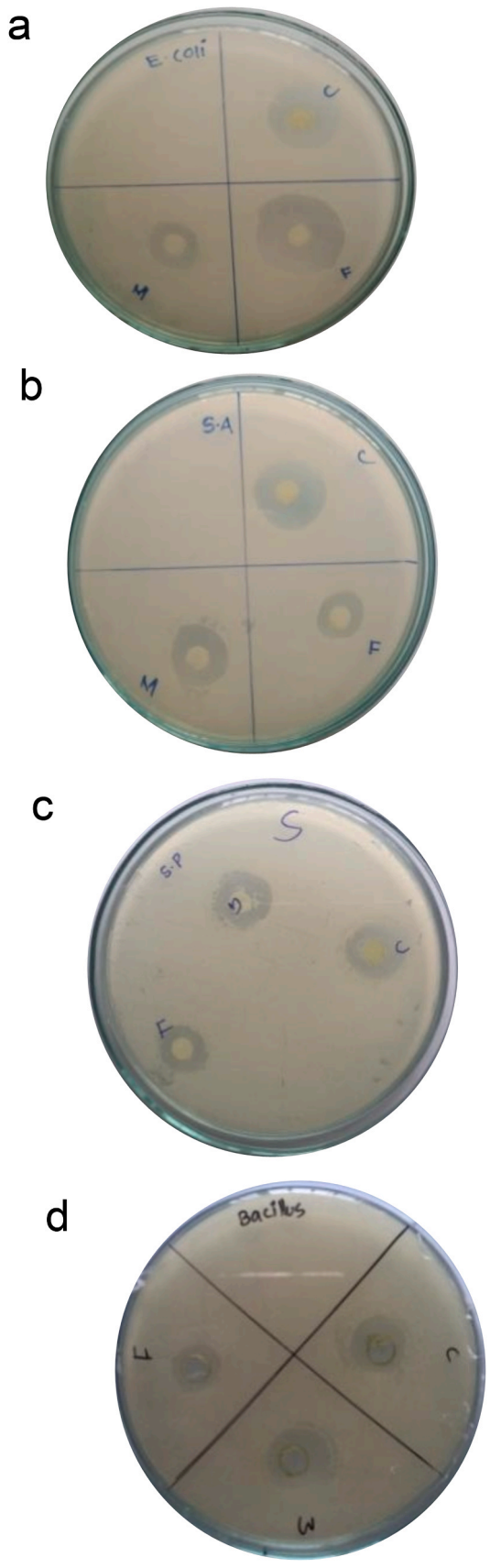

Fig. 5. Antibacterial assay (a) *E. coli* (b) *Pseudomonas sp.* (c) *Vibrio sp.* (d) *Bacillus sp.*

E. coli, *S. aureus*, *Klebsiella sp.*, and *Bacillus subtilis* [46], while *Cucumis maderaspatanus*-derived ZnO NPs exhibited significant antibacterial and photocatalytic properties [43]. Such findings corroborate with the antimicrobial efficacy observed in this study.

According to [79], the MIC and MBC values of *E. granulata*-mediated AgNPs demonstrated significant resistance against pathogens such as *S. aureus* and *E. coli*, which is consistent with the efficacy observed in our study using ZnO NPs. Our findings indicated that ZnO NPs exhibited remarkable antibacterial activity, particularly against *E. coli*, with an inhibition zone of 13 mm. The antibacterial action is attributed to the generation of toxic oxygen radicals that damage bacterial cell membranes, along with the electrostatic interaction between the negatively charged bacteria and the positively charged ZnO particles, leading to bacterial cell death [43]. In the previous research [76] *Digera muricata* mediated ZnO NPs reports a potential antibacterial effect against *E. coli*, *S. aureus*, *S. faecalis*, *K. pneumoniae*, *P. aeruginosa*, and *B. subtilis,* with the zone of inhibition in the range 7–33 mm.

Similarly, *E. petiolata*-mediated ZnO NPs were found to exhibit significant antibacterial activity against *E. coli*, with an inhibition zone of 12 mm, surpassing the effectiveness of the antibiotic chloramphenicol [80]. The antibacterial activities of ZnO NPs are also enhanced by their dispersibility in water, which facilitates their role in reducing waterborne diseases and preventing bacterial contamination [81]. ZnO NPs derived from mint leaves have shown strong antibacterial effects against *P. aeruginosa* and *E. coli*, highlighting their potential use in food preservation. These nanoparticles could be incorporated into food packaging materials to inhibit microbial growth, thus extending the shelf life of food products [50];[82].

Moreover, the role of ZnO NPs in enhancing antibacterial efficacy was examined under heavy metal stress, where the antibacterial effect against *Bacillus sp.* was linked to wastewater remediation [83]. In a similar context, *Calotropis procera*-synthesized ZnO NPs demonstrated the ability to reduce populations of *Vibrio cholerae*, an aquatic-borne pathogen responsible for gastrointestinal infections and diarrheal diseases. The antibacterial action was associated with membrane disruption and reactive oxygen species (ROS) generation, further confirming the potential of ZnO NPs in combating aquatic pathogens [84];[85]. The antibacterial activity of ZnO nanoparticles occurs through three key mechanisms such as generation of reactive oxygen species (ROS), direct interaction with bacterial membranes, and release of Zn^{2+} ions. ZnO NPs induce oxidative stress by generating ROS such as hydroxyl radicals (OH), superoxide anions (O_2^-), and hydrogen peroxide (H_2O_2). These reactive species damage bacterial proteins, lipids, and DNA, leading to cell death [50]. The positive surface charge of ZnO NPs interacts electrostatically with negatively charged bacterial membranes, disrupting membrane integrity, increasing permeability, and causing cytoplasmic leakage [51]. ZnO NPs also release Zn^{2+} ions that penetrate bacterial cells, interfere with enzymatic activities, and disrupt intracellular metabolic pathways, resulting in bacterial inhibition [81].

This study demonstrates that ZnO NPs exhibit substantial antibacterial activity against a variety of aquatic pathogens, thereby offering a means to prevent bacterial infections in fish and other aquatic organisms. Their efficacy in controlling waterborne pathogens positions ZnO NPs as a promising alternative to traditional antibiotics, helping to mitigate the proliferation of drug-resistant bacteria in aquatic ecosystems. Furthermore, the incorporation of ZnO NPs into fish feed holds the potential to enhance the immune response of aquatic organisms, contributing to improved health management and sustainability in aquaculture.

5. Conclusion

The utilization of *E. antiquorum* for the green synthesis of ZnO NPs offers a potential and sustainable method for producing nanoparticles. The XRD, FT-IR, EDX, and FE-SEM studies were used to describe the morphology and structure of ZnO NPs manufactured using a green

method. The XRD examination revealed that the crystallite size was 37 nm. The ZnO NPs were characterized as having a nanoflake structure. The size of the nanoparticles ranged from 500 nm to 56 nm and from 2 μm to 16 nm, as determined by SEM analysis. The MIC and MBC concentrations of ZnO nanoparticles biosynthesized from *E. antiquorum* exhibit significant antibacterial effects. Therefore, ZnO NPs has potential antibacterial efficacy against aquatic-borne pathogens which prevent bacterial infections. This method utilizes the inherent stabilizing and reducing chemicals found in the plant, offering an environmentally acceptable substitute for conventional synthesis processes. The biosynthesis method of ZnO NPs, obtained from *E. antiquorum*, represents a significant improvement in nanoparticle production, primarily due to its environmentally sensitive approach. The ZnO NPs obtained have a wide range of uses in various fields such as biomedical devices and the food industry, showcasing the potential of plant-based nanotechnology in multiple domains. Hence, this study concluded that synthesized ZnO NPs have the potential to be bactericidal, and eradicate waterborne diseases. ZnO NPs are capable of enhancing fish immunity, which may result in improved aquaculture health and greater sustainability.

CRediT authorship contribution statement

Surya Sivakumar: Methodology, Validation, Formal analysis. **Boobal Rangaswamy:** Conceptualization, Methodology, Validation, Formal analysis, Visualization, Data curation, Writing – original draft, Writing –review & editing, Supervision, Investigation. **Lathika Shanmugam:** Data Curation, Visualization, Writing - Original Draft, Writing - Review & Editing. **Kamalesh Marudhachalam:** Writing - Original Draft, Writing - Review & Editing.

Declaration of Competing Interest

The authors declare that they have no known competing financial interests or personal relationships that could have appeared to influence the work reported in this paper.

Informed consent statement

Not applicable.

Consent to publish

All authors approved the manuscript and gave their consent for submission and publication.

Data availability

There is no research related data stored in publicly available repositories, and the data will be made available on request.

References

[1] C.M. Rico, S. Majumdar, M. Duarte-Gardea, J.R. Peralta-Videa, J.L. Gardea-Torresdey, Interaction of nanoparticles with edible plants and their possible implications in the food chain, J. Agric. Food Chem. 59 (2011) 3485–3498. https://pubs.acs.org/doi/10.1021/jf104517j.

[2] M. Munir, S. Hussain, R. Anwar, M. Waqas, J.A. Online, The role of nanoparticles in the diagnosis and treatment of diseases (Available from:), Sci. Inq. Rev. (SIR) [Internet] 4 (3) (2020), https://doi.org/10.32350/sir.43.02.

[3] U. Ikoba, H. Peng, H. Li, C. Miller, C. Yu, Q. Wang, Nanocarriers in therapy of infectious and inflammatory diseases, Nanoscale 7 (10) (2015) 4291–4305, https://doi.org/10.1039/C4NR07682F.

[4] A.R. Lowery, A.M. Gobin, E.S. Day, N.J. Halas, J.L. West, Immunonanoshells for targeted photothermal ablation of tumor cells, Int. J. Nanomed. 1 (2) (2006) 149–154, https://doi.org/10.2147/nano.2006.1.2.149.

[5] P. Nasimi, M. Haidari, Medical use of nanoparticles: drug delivery and diagnosis diseases, Int. J. Green Nanotechnol. 5 (1) (2013) 1–5, https://doi.org/10.1177/1943089213506978.

[6] H. Rehman, Z. Ali, M. Hussain, S.R. Gilani, T.G. Shahzady, A. Zahra, et al., Synthesis and characterization of zno nanoparticles and their use as an adsorbent for the arsenic removal from drinking water, Digest J. Nanomater. Biostruct. 14 (2019).

[7] S. Iravani, Green synthesis of metal nanoparticles using plants, Jan 10, Green Chem 13 (10) (2011) 2638–2650, https://doi.org/10.1039/C1GC15386B.

[8] J.Y. Song, B.S. Kim, Rapid biological synthesis of silver nanoparticles using plant leaf extracts, Jan, Bioprocess Biosyst. Eng. 31 (1) (2009) 79–84, https://doi.org/10.1007/s00449-008-0224-6.

[9] P. Deka, K.K. Nath, S.K. Borthakur, Ethoiatrical uses of Euphorbia antiquorum L. and E. ligularia Roxb. in Assam, Indian J. Tradit. Knowl. 7 (2008).

[10] O. Abiodoun Pascal, A. Erick Virgyle Bertrand, A. Yatchégnon Eloi, C. Olounladé Abiodoun Pascal, T. Esaïe, H.A. Mawulé Sylvie, A review of the ethnomedical uses, phytochemistry and pharmacology of the Euphorbia genus, Journal [Internet] 6 (1) (2017) 34–93. Available from: www.thepharmajournal.com.

[11] M. Aleksandrov, V. Maksimova, L.K. Gudeva, Review of the anticancer and cytotoxic activity of some species from genus euphorbia, Agric. Conspec. Sci. 84 (2019).

[12] Y. Shen, L. Zhang, K. Wang, X. Li, J. Li, S. Zhang, et al., Bio-mediated synthesis – A sustainable strategy for nanomaterials preparation: a comprehensive bibliometric review, Nano Sel. 2 (12) (2021 Dec 9) 2275–2290.

[13] N. Shreyash, S. Bajpai, A. Khan Mohd, Y. Vijay, S.K. Tiwary, M. Sonker, Green Synthesis of Nanoparticles and Their Biomedical Applications: A Review, ACS Appl Nano Mater [Internet] 4 (11) (2021) 11428–11457. Available from: https://pubs.acs.org/doi/10.1021/acsanm.1c02946.

[14] Rai S. Biomedical applications of green synthesized cerium oxide nanoparticles. In 2024. p. 173–196.Available from: https://mrforum.com/product/9781644903278-7.

[15] K. Deepak Raj SCKKA. Current developments in the synthesis of nanoparticles using plant extracts. 2025.

[16] H.N. Jayasimha, K.G. Chandrappa, P.F. Sanaulla, V.G. Dileepkumar, Green synthesis of CuO nanoparticles: A promising material for photocatalysis and electrochemical sensor, Jan 1, Sens. Int. [Internet] 5 (2024) 100254. Available from: https://linkinghub.elsevier.com/retrieve/pii/S2666351123000281.

[17] J. Mou, Y. Ren, J. Wang, C. Wang, Y. Zou, K. Lou, et al., Nickel oxide nanoparticle synthesis and photocatalytic applications: evolution from conventional methods to novel microfluidic approaches, Apr 9, Microfluid Nanofluidics [Internet] 26 (4) (2022) 25. Available from: https://link.springer.com/10.1007/s10404-022-02534-2.

[18] N.D. Jaji, H.L. Lee, M.H. Hussin, H.M. Akil, M.R. Zakaria, M.B.H. Othman, Advanced nickel nanoparticles technology: From synthesis to applications, Dec 31, Nanotechnol Rev [Internet] 9 (1) (2020) 1456–1480. Available from: https://www.degruyter.com/document/doi/10.1515/ntrev-2020-0109/html.

[19] Y. Cao, H.J. Wang, C. Cao, Y.Y. Sun, L. Yang, Y.N. Zhang, Synthesis and anti-ultraviolet properties of monodisperse BSA-conjugated zinc oxide nanoparticles, Jan 31, Mater Lett [Internet] 65 (2) (2011) 340–342. Available from: https://linkinghub.elsevier.com/retrieve/pii/S0167577X10009067.

[20] J. Singh, T. Dutta, K.H. Kim, M. Rawat, P. Samddar, P. Kumar, 'Green' synthesis of metals and their oxide nanoparticles: applications for environmental remediation, Dec 30, J Nanobiotechnology [Internet] 16 (1) (2018) 84. Available from: https://jnanobiotechnology.biomedcentral.com/articles/10.1186/s12951-018-0408-4.

[21] P. Kumar Sake, V.L. Reddy, S.P. Valli Khan, Isolation and quantification of flavonoid from euphorbia antiquorum latex and its antibacterial studies, Indian J. Adv. Chem. Sci. 1 (2013).

[22] S. Sabir, M. Arshad, S.K. Chaudhari, Zinc Oxide Nanoparticles for Revolutionizing Agriculture: Synthesis and Applications, The Scientific World Journal [Internet] 2014 (2014) 1–8. Available from, ⟨http://www.hindawi.com/journals/tswj/2014/925494/⟩.

[23] K. Omri, I. Najeh, R. Dhahri, J. El Ghoul, L. El Mir, Effects of temperature on the optical and electrical properties of ZnO nanoparticles synthesized by sol–gel method, Microelectron Eng [Internet] 128 (2014 Oct 5) 53–58. Available from, ⟨https://linkinghub.elsevier.com/retrieve/pii/S0167931714002366⟩.

[24] Ali A. Annu, S. Ahmed, Green Synthesis of Metal, Metal Oxide Nanoparticles, and Their Various Applications. Handbook of Ecomaterials [Internet], Springer International Publishing, Cham, 2018, pp. 1–45. Available from, ⟨http://link.springer.com/10.1007/978-3-319-48281-1_115-1⟩.

[25] M.S. Geetha, H. Nagabhushana, H.N. Shivananjaiah, Green mediated synthesis and characterization of ZnO nanoparticles using Euphorbia Jatropa latex as reducing agent, Journal of Science: Advanced Materials and Devices [Internet] 1 (3) (2016 Sep 1) 301–310. ⟨https://linkinghub.elsevier.com/retrieve/pii/S2468217916300156⟩.

[26] M. Manokari, M.S. ShekhawatEcofriendly synthesis of Zinc oxide nanoparticles from asthma plant-Euphorbia hirta L. 2017; Available from: www.worldscientificnews.com.

[27] G. Durga Devi, K. Murugan, C. Panneer SelvamHelicoverpa armigera (Lepidoptera: Noctuidae). Vol. 5, Euphorbia hirta silver nanopaticles JBiopest. 2014..

[28] N.R. Ramli, H.M. Yusoff, M. Maulidiani, A. Asari, N. Huda, A. Wahab, Stability of green synthesis of silver nanoparticles by using Euphorbia milii (EUPHORBIACEAE) leaves extract with different solvents and polarities (Kestabilan Sintesis Hijau Nanopartikel Perak dari Ekstrak Daun Euphorbia milii (Euphorbiaceae) menggunakan Pelarut dan Kekutuban yang Berbeza), Malays. J. Anal. Sci. 27 (2023).

[29] A. Barzinjy, Characterization of ZnO Nanoparticles Prepared from Green Synthesis Using Euphorbia Petiolata Leaves, Eurasian Journal of Science and Engineering [Internet] 4 (3) (2019). Available from: ⟨https://eajse.tiu.edu.iq/index.php/eajse/article/view/284⟩.

[30] C. Rajkuberan, S. Prabukumar, G. Sathishkumar, A. Wilson, K. Ravindran, S. Sivaramakrishnan, Facile synthesis of silver nanoparticles using Euphorbia antiquorum L. latex extract and evaluation of their biomedical perspectives as anticancer agents, Journal of Saudi Chemical Society [Internet] 21 (8) (2017 Dec 1) 911–919. ⟨https://linkinghub.elsevier.com/retrieve/pii/S1319610316000041⟩.

[31] M. Snehal Yedurkar, D. Kapil Punjabi, B. Chandra Maurya, A. Prakash Mahanwar, Biosynthesis of Zinc Oxide Nanoparticles using Euphorbia Milii Leaf Extract- A Green Approach, Mater Today Proc [Internet] 5 (10) (2018) 22561–22569. Available from, ⟨https://linkinghub.elsevier.com/retrieve/pii/S2214785318317620⟩.

[32] N.M. Muchanyereyi, T. Muchenje, S. Nyoni, M. Shumba, M. Mupa, L. Gwatidzo, et al., Green synthesis of silver nanoparticles using euphorbia confinalis stem extract, characterization and evaluation of antimicrobial activity, J. Nanomater. Mol. Nanotechnol 06 (03) (2017). Available from, ⟨https://www.scitechnol.com/peer-review/green-synthesis-of-silver-nanoparticles-using-euphorbia-confinalis-stem-extract-characterization-and-evaluation-of-antimicrobial-a-qwjC.php?article_id=6138⟩.

[33] H.I. Abd El-Moaty, E.H. Ismail, R. Abu-Khudir, N.A. Soliman, D.Y. Sabry, N.K. Al Abdulsalam, et al., Characterization and evaluation of multiple biological activities of phytosynthesized gold nanoparticles using aqueous extract of Euphorbia dendroides, Nanomater. Nanotechnol 12 (2022). Jan 30;12: 184798042211412. Available from, ⟨http://journals.sagepub.com/doi/10.1177/18479804221141266⟩.

[34] K. Roy, A.K. Srivastwa, C.K. Ghosh, Anticoagulant, thrombolytic and antibacterial activities of Euphorbia acruensis latex-mediated bioengineered silver nanoparticles, Green Process. Synth. 8 (1) (2019) 590–599.

[35] Bawazeer. Green synthesis of silver nanoparticles from Euphorbia milii plant extract for enhanced antibacterial and enzyme inhibition effects. 2024.

[36] S.V. Patil, H.P. Borase, C.D. Patil, B.K. Salunke, Biosynthesis of silver nanoparticles using latex from few euphorbian plants and their antimicrobial potential, Appl. Biochem Biotechnol. 167 (4) (2012) 776–790.

[37] Y. Sadeghipour, M.H. Alipour, H.R.G. Jafarbeigloo, A. Salahvarzi, M. Mirzaii, A. mohammad Amani, et al., Evaluation antibacterial activity of biosynthesized silver nanoparticles using e euphorbia pseudocactus berger extracts (Euphorbiaceae), Nanomed. Res. J. 5 (3) (2020) 265–275.

[38] Elumalai E.K., Prasad T.N.V.K. V, Hemachandran J., Therasa S.V., Thirumalai T., David E. Extracellular synthesis of silver nanoparticles using leaves of Euphorbia hirta and their antibacterial activities. 2010.

[39] M. Arif, R. Ullah, M. Ahmad, A. Ali, Z. Ullah, M. Ali, et al., Green synthesis of silver nanoparticles using euphorbia wallichii leaf extract: its antibacterial action against citrus canker causal agent and antioxidant potential, Molecules 27 (11) (2022). Available from, ⟨https://www.mdpi.com/1420-3049/27/11/3525⟩.

[40] S. Mehr-Un-nisa, Y.M. Jan, Z.H. Khan, A.K. Shah, A.K. Azad, Balaraman, Synthesis and biological potential of sliver nanoparticles of euphorbia helioscopia L, Curr. Trends Biotechnol. Pharm 17 (1) (2023) 621–626. Available from, ⟨https://abap.co.in/index.php/home/article/view/752⟩.

[41] S.S. Oliveira, G.C. Braga, N.K. Cordeiro, J.R. Stangarlin, H.J. Alves, Green synthesis of silver nanoparticles with Euphorbia tirucalli extract and its protection against microbial decay of strawberries during storage, J. Food Sci. Technol. 59 (5) (2022) 2025–2034.

[42] Abduljabbara, Selenium nanoparticles from Euphorbia retusa extract and its biological applications: antioxidant, and antimicrobial activities, Egypt J. Chem. 0 (0) (2024) 0–0. Available from: ⟨https://ejchem.journals.ekb.eg/article_310430.html⟩.

[43] M. Gurusamy, M. Sellavel, V.B. Kuppuvelsamy, A sustainable green synthesis for photocatalytic and antibacterial activity of zinc oxide nanoparticles using Cucumis maderaspatanus leaf extract, Desalin. Water Treat 319 (2024). Available from, ⟨https://ejchem.journals.ekb.eg/article_310430.html⟩.

[44] N. Ahmad, M. Fozia, Z.U. Jabeen, I. Haq, A. Ahmad, Wahab, et al., Green fabrication of silver nanoparticles using euphorbia serpens kunth aqueous extract, their characterization, and investigation of its in vitro antioxidative, antimicrobial, insecticidal, and cytotoxic activities. Biomed. Res. Int. 2022, 2022. Available from, ⟨https://onlinelibrary.wiley.com/doi/10.1155/2022/5562849⟩.

[45] U. Khattak, R. Ullah, S. Ali Khan, S. Afriq Jan, A. Rauf, M. Fawzy Ramadan, Synthesis, characteristics and biological activities of silver nanoparticles from Euphorbia dracunculoides, Eurasia J. Biosci. Eurasia J. Biosci. 13 (2019).

[46] G. Venkatesh, G. Serdaroğlu, E. Üstün, D. Haripriya, P. Vennila, V. Siva, et al., Green synthesis, characterization, anti-cancer and antimicrobial activity of AuNPs extracted from Euphorbia antiquorum stem and flower: experimental and theoretical calculations, J. Drug Deliv. Sci. Technol 95 (2024). Available from, ⟨https://linkinghub.elsevier.com/retrieve/pii/S1773224724002521⟩.

[47] A.R. Phull, A. Ali, A. Ali, S. Abbasi, M. Zia, M.H. Khaskheli, et al., Synthesis of silver nanoparticles using euphorbia wallichii extract and assessment of their bio-functionalities, Med Chem 16 (4) (2019). Available from, ⟨https://www.eurekaselect.com/176561/article⟩.

[48] H.A. Ghramh, K.A. Khan, E.H. Ibrahim, Biological activities of Euphorbia peplus leaves ethanolic extract and the extract fabricated gold nanoparticles (AuNPs), Molecules 24 (7) (2019).

[49] J. Prakash, K. Vignesh, T. Anusuya, T. Kalaivani, C. Ramachandran, R. Sudha Rani, Momna Rubab, et al. Application of Nanoparticles in Food Preservation and Food Processing, Journal of Food Hygiene and Safety [Internet] 34 (4) (2019 Aug 31) 317–324. ⟨http://foodsafety.or.kr/journal/article.php?code=67967⟩.

[50] S. Sirelkhatim, S. Mahmud, A. Seeni, N.H.M. Kaus, L.C. Ann, S.K.M. Bakhori, et al., Review on zinc oxide nanoparticles: Antibacterial activity and toxicity mechanism, NanoMicro Lett 7 (2015) 219–242. ⟨http://link.springer.com/10.1007/s40820-015-0040-x⟩.

[51] K.R. Raghupathi, R.T. Koodali, A.C. Manna, Size-dependent bacterial growth inhibition and mechanism of antibacterial activity of zinc oxide nanoparticles, Langmuir 27 (7) (2011) 4020–4028. Available from, ⟨https://pubs.acs.org/doi/10.1021/la104825u⟩.

[52] R. Verma, S. Pathak, A.K. Srivastava, S. Prawer, S. Tomljenovic-Hanic, ZnO nanomaterials: green synthesis, toxicity evaluation and new insights in biomedical applications, in: Journal of Alloys and Compounds, 876, Elsevier Ltd, 2021. ⟨https://linkinghub.elsevier.com/retrieve/pii/S092583882101584X⟩.

[53] S. Vijaya Bharathi, M. Das, Cytotoxicity effect of nanoparticles of Euphorbia antiquorum on breast cancer cell line, South Afr. J. Bot 151 (2022). Available from, ⟨https://linkinghub.elsevier.com/retrieve/pii/S0254629922005440⟩.

[54] M. Bandeira, M. Giovanela, M. Roesch-Ely, D.M. Devine, J. Da, S. Crespo, Green synthesis of zinc oxide nanoparticles: a review of the synthesis methodology and mechanism of formation (2020). Available from, ⟨https://linkinghub.elsevier.com/retrieve/pii/S2352554119301068⟩.

[55] M. Manokari, M.S. Shekhawat, Ecofriendly synthesis of Zinc oxide nanoparticles from asthma plant-Euphorbia hirta L, World Sci News [Internet] (2017). Available from, ⟨www.worldscientificnews.com⟩.

[56] D. Mahendiran, G. Subash, D. Arumai Selvan, D. Rehana, R. Senthil Kumar, A. Kalilur Rahiman, Biosynthesis of zinc oxide nanoparticles using plant extracts of aloe vera and hibiscus sabdariffa: phytochemical, antibacterial, antioxidant and anti-proliferative studies, Bionanoscience 7 (3) (2017) 530–545. Available from, ⟨http://link.springer.com/10.1007/s12668-017-0418-y⟩.

[57] F.N. Alharbi, Z.M. Abaker, S.Z.A. Makawi, Phytochemical substances—mediated synthesis of zinc oxide nanoparticles (ZnO NPS), Aug 5, Inorganics (Basel) [Internet] 11 (8) (2023) 328. Available from: https://www.mdpi.com/2304-6740/11/8/328.

[58] K.D. Rajesh, Qualitative and quantitative phytochemical analysis in four pteridophytes. Int. J. Pharm. Sci. Rev. Res. 27 (2014). Available from: www.globalresearchonline.net.

[59] S.S.M. Hassan, W.I.M.E. Azab, H.R. Ali, M.S.M. Mansour, Green synthesis and characterization of ZnO nanoparticles for photocatalytic degradation of anthracene, Adv. Nat. Sci. Nanosci. Nanotechnol 6 (4) (2015). Available from, ⟨https://iopscience.iop.org/article/10.1088/2043-6262/6/4/045012⟩.

[60] Cullity, Elements of X-Ray Diffraction, Pearson Education Limited, 2014, p. 608.

[61] D. Geetha, T. Thilagavathi, Hydrothermal synthesis of nano ZnO Structures from CTAB, Dig. J. Nanomater. Biostruct. 5 (2010).

[62] H. Sarma, K.C. Sarma, B.N. College, A. Dhubri, X-ray peak broadening analysis of ZnO nanoparticles derived by precipitation method, Int. J. Sci. Res. Publ. [Internet] 4 (3) (2014). Available from, ⟨www.ijsrp.org⟩.

[63] M.A. Hossain, M.A. Hossain, Synthesis of carbon nanoparticles from kerosene and their characterization by SEMÆDX, XRD and FTIR, Am. J. Nanosci. Nanotechnol. 1 (2) (2013) 52. Available from: http://www.sciencepublishinggroup.com/journal/paperinfo.aspx?journalid=226&doi=10.11648/j.nano.20130102.12.

[64] N. Korkmaz, Y. Ceylan, R. İmamoğlu, D. Kısa, F. Şen, A. Karadağ, Eco-friendly biogenic silver nanoparticles: synthesis, characterization and biological applications, Int. J. Environ. Sci. Technol (2024). Available from, ⟨https://link.springer.com/10.1007/s13762-024-05860-w⟩.

[65] S. Pradeep, S.C. Prabhuswaminath, P. Reddy, S.M. Srinivasa, A.A. Shati, M. Y. Alfaifi, et al., Anticholinesterase activity of Areca catechu: in vitro and in silico green synthesis approach in search for therapeutic agents against Alzheimer's disease, Front. Pharmacol 13 (2022). Available from, ⟨https://www.frontiersin.org/articles/10.3389/fphar.2022.1044248/full⟩.

[66] S. Srivastava, D. Panchani, N. Modi, Phytochemical analysis of euphorbia species of gujarat, india: a review, Int. Assoc. Biol. Comput. Dig. 3 (1) (2024) 22–33. Available from, ⟨https://iabcd.org.in/index.php/iabcd/article/view/195⟩.

[67] N. Bhardwaj, B. Goel, N. Tripathi, B. Sahu, S.K. Jain, A comprehensive review on chemistry and pharmacology of marine bioactives as antimetastatic agents, Eur. J. Med. Chem. Rep. 4 (2022). Available from, ⟨https://linkinghub.elsevier.com/retrieve/pii/S2772417421000236⟩.

[68] L. Abdel-Ghany Refahy, Study on flavonoids and triterpenoids content of some euphorbiaceae plants, J. Life Sci. 5 (2011).

[69] E.M. Abdallah, Antimicrobial properties and phytochemical constituents of the metha-nol extracts of *Euphorbia retusa* Forssk. and *Euphorbia terracina* L. from Saudi Arabia, South Asian J. Exp. Biol 4 (2) (2014) 48–53. Available from, ⟨https://sajeb.org/index.php/sajeb/article/view/156⟩.

[70] Okeniyi, Phytochemical screening, cytotoxicity, antioxidant and antimicrobial activities of stem and leave extracts of euphorbia heterophylla, J. Biol. Life Sci. 4 (1) (2012). Available from: ⟨http://www.macrothink.org/journal/index.php/jbls/article/view/2047⟩.

[71] J.N. Ogbulie, C.C. Ogueke, I.C. Okoli, B.N. Anyanwu, Antibacterial activities and toxicological potentials of crude ethanolic extracts of Euphorbia hirta, Afr. J. Biotechnol 6 (13) (2007) 1544–1548. Available from: ⟨http://www.academicjournals.org/AJB⟩.

[72] F. Hassan, Synthesis of Nickel Nanoparticles Using Poly(vinyl alcohol) as a Capping Agent [Internet] (2015). Available from, ⟨https://www.researchgate.net/publication/281677595⟩.

[73] R. Yuvakkumar, J. Suresh, B. Saravanakumar, A. Joseph Nathanael, S.I. Hong, V. Rajendran, Rambutan peels promoted biomimetic synthesis of bioinspired zinc oxide nanochains for biomedical applications, Spectrochim. Acta A Mol. Biomol. Spectrosc 137 (2015) 250–258. Available from, ⟨https://linkinghub.elsevier.com/retrieve/pii/S138614251401213X⟩.

[74] S. Siva Kumar, P. Venkateswarlu, V. Ranga Rao, G. Nageswara Rao, Synthesis, characterization and optical properties of zinc oxide nanoparticles [Internet] (2013). Available from, ⟨http://www.inl-journal.com/content/3/1/30⟩.

[75] M.U. Rashid, S.J. Shah, S. Attacha, L. Khan, J. Saeed, S.T. Shah, et al., Green synthesis and characterization of zinc oxide nanoparticles using citrus limetta peels extract and their antibacterial activity against brown and soft rot pathogens and antioxidant potential, Waste Biomass. Valoriz 15 (6) (2024) 3351–3366. Available from, ⟨https://link.springer.com/10.1007/s12649-023-02389-w⟩.

[76] N. Ashraf, S.H. Sumrra, M.A. Assiri, M. Usman, R. Hussain, F. Aziz, et al., *Digera muricata* (L.) Mart. mediated synthesis of antimicrobial and enzymatic inhibitory zinc oxide bionanoparticles, Green Process. Synth 10 (1) (2021) 476–484. Available from, ⟨https://www.degruyter.com/document/doi/10.1515/gps-2021-0044/html⟩.

[77] J.M. Yousef, E.N. Danial, In *Vitro* antibacterial activity and minimum inhibitory concentration of zinc oxide and nano-particle zinc oxide against pathogenic strains, Int. J. Health Sci. 2 (4) (2012) 38–42. Available from, ⟨http://article.sapub.org/10.5923.j.health.20120204.04.html⟩.

[78] R. Wahab, A. Mishra, S. Il Yun, I.H. Hwang, J. Mussarat, A.A. Al-Khedhairy, et al., Fabrication, growth mechanism and antibacterial activity of ZnO micro-spheres prepared via solution process, Biomass. Bioenergy 39 (2012) 227–236. Available from, ⟨https://linkinghub.elsevier.com/retrieve/pii/S0961953412000062⟩.

[79] G. Periyasami, S. Palaniappan, P. Karuppiah, M. Rahaman, P. Karthikeyan, A. Aldalbahi, et al., Biogenic silver nanoparticles fabricated by euphorbia granulata forssk's extract: investigating the antimicrobial, radical scavenging, and catalytic activities. J. Nanomater 2022, 2022. Available from, ⟨https://onlinelibrary.wiley.com/doi/10.1155/2022/3864758⟩.

[80] C. Mohammadi, S.A. Mahmud, S.M. Abdulla, Y. Mirzaei, Moroccan Journal of Chemistry Green synthesis of ZnO nanoparticles using the aqueous extract of Euphorbia petiolata and study of its stability and antibacterial properties [Internet], J. Chem 5 (2017). ⟨http://revues.imist.ma/?journal=morjchem&page=login⟩.

[81] J. Sawai, Quantitative evaluation of antibacterial activities of metallic oxide powders (ZnO, MgO and CaO) by conductimetric assay, J. Microbiol. Methods 54 (2) (2003 Aug 1) 177–182. Available from, ⟨https://linkinghub.elsevier.com/retrieve/pii/S016770120300037X⟩.

[82] P. Joshi, S. Chakraborti, P. Chakrabarti, D. Haranath, V. Shanker, Z.A. Ansari, et al., Role of surface adsorbed anionic species in antibacterial activity of ZnO quantum dots against Escherichia coli, J. Nanosci. Nanotechnol 9 (11) (2009) 6427–6433. Available from, ⟨http://openurl.ingenta.com/content/xref?genre=article&issn=1533-4880&volume=9&issue=11&spage=6427⟩.

[83] N. Akhtar, S. Khan, S.U. Rehman, Z.U. Rehman, Z.U.R. Mashwani, E.S. Rha, et al., Zinc oxide nanoparticles enhance the tolerance and remediation potential of bacillus spp. against heavy metal stress, Adsorpt. Sci. Technol. 2021 (2021). Available from, ⟨http://journals.sagepub.com/doi/10.1155/2021/1774528⟩.

[84] W. Salem, D.R. Leitner, F.G. Zingl, G. Schratter, R. Prassl, W. Goessler, et al., Antibacterial activity of silver and zinc nanoparticles against Vibrio cholerae and enterotoxic Escherichia coli, Int. J. Med. Microbiol 305 (1) (2015) 85–95. Available from, ⟨https://linkinghub.elsevier.com/retrieve/pii/S1438422114001532⟩.

[85] S. Sarwar, S. Chakraborti, S. Bera, I.A. Sheikh, K.M. Hoque, P. Chakrabarti, The antimicrobial activity of ZnO nanoparticles against Vibrio cholerae: variation in response depends on biotype, Nanomedicine 12 (6) (2016) 1499–1509. Available from, ⟨https://linkinghub.elsevier.com/retrieve/pii/S1549963416000952⟩.